JOURNAL OF SOLID STATE CHEMISTRY 109, 53–59 (1994)

Synthesis of $LiTiPO_5$ and $LiTiAsO_5$ with the α-Fe_2PO_5 Structure

A. Robertson, J. G. Fletcher, J. M. S. Skakle, and A. R. West

Department of Chemistry, University of Aberdeen, Meston Walk, Aberdeen AB9 2UE, United Kingdom

Received February 2, 1993; in revised form June 8, 1993; accepted June 16, 1993

The new phases $LiTiPO_5$ and $LiTiAsO_5$ have been synthesized by solid state reaction. They are essentially isostructural with α-Fe_2PO_5, as confirmed by X-ray Rietveld refinement. The structures are built of chains of edge-sharing LiO_6 octahedra cross-linked by chains of alternate corner-sharing PO_4 tetrahedra and TiO_6 octahedra (each of which shares common faces with two LiO_6 octahedra). Unit cell dimensions: $LiTiPO_5$, a = 7.4000(5) Å, b = 6.3752(3) Å, c = 7.2347(4) Å; $LiTiAsO_5$, a = 7.5257(5) Å, b = 6.5786(4) Å, c = 7.4524(5) Å. Space group: *Pnma*. The phases melt incongruently at ~1080°C and exhibit very low electrical conductivities, (5–10) × 10^{-6} S cm^{-1} at 400°C with activation energy ~1 eV. Subsolidus phase diagrams for the systems Li_2O–TiO_2–P_2O_5/As_2O_5 are presented.

INTRODUCTION

There is currently much interest in a Li^+ ion conducting lithium titanium phosphate for possible solid electrolyte applications (1–11). The phase of interest has the formula $LiTi_2(PO_4)_3$ but, in order to obtain high conductivity, certain additives are necessary, especially Al or Sc (4, 6, 8, 10, 11). The reasons for the enhanced conductivity are still not fully clear. Suggestions have been made of either a lithium interstitial mechanism associated with the substitution,

$$Ti^{4+} \rightleftharpoons Li^+ + Al^{3+}$$

or a composite effect in which the conductivity of the surface of the $LiTi_2(PO_4)_3$ grains is enhanced by the presence of an insulating second phase.

During a study to investigate the stoichiometry and properties of $LiTi_2(PO_4)_3$, we carried out a partial phase diagram study of the system Li_2O–TiO_2–P_2O_5, during which the new phase $LiTiPO_5$ was encountered. Here we report its structure and properties together with those of its analogue, $LiTiAsO_5$.

EXPERIMENTAL

Reagents used were Li_2CO_3, TiO_2, $NH_4H_2PO_4$, and As_2O_5 (all ANALAR). All were used direct from the bottle except TiO_2 which was dried at 600°C. Samples were weighed out, ground together with acetone to form a paste using an agate mortar and pestle, dried, and fired in Au boats. Samples were initially heated at 200°C for half an hour, then the temperature was gradually increased to 650°C and kept at this temperature for 1–2 hr. Samples were reground and fired at 800–1000°C for 1–2 days.

Using these conditions no significant volatilization of reagents occurred, as determined by weight loss checks. For X-ray powder diffraction a Hägg Guinier camera ($CuK\alpha_1$ radiation) was used for general phase identification. For accurate lattice parameter determination and the recording of intensity data for Rietveld refinements, a STOE STADI P diffractometer was used in transmission mode with a small linear position sensitive detector (psd), Ge monochromator, and $CuK\alpha_1$ radiation. The 2θ range of the psd was ~7° with a step width of 2°. For accurate lattice parameters, Si was added as an internal standard. For Rietveld refinements, data were collected over the range $5 \leq 2\theta \leq 110°$, count time 1200 sec/step. Conductivities were measured on sintered pellets, with Au electrodes, by ac impedance methods.

RESULTS AND DISCUSSION

The new phases: $LiTiPO_5$ and $LiTiAsO_5$, were readily prepared by solid state reaction at 950°C and 850°C, respectively. The phases are white and pale yellow, melt at 1085 ± 20 and 1075 ± 20°C, respectively, and are stable in air. Melting appears to be incongruent from analysis of the products present in samples quenched from just above the melting temperatures. These were, for $LiTiPO_5$: $LiTi_2(PO_4)_3$, TiO_2 + unidentified phase(s) and for $LiTiAsO_5$: βLi_3AsO_4, TiO_2 + unidentified phase(s). In both cases there was little evidence of the original $LiTiPO_5$ and $LiTiAsO_5$.

The X-ray powder diffraction data were indexed on orthorhombic unit cells using a trial and error procedure included in the STOE software package. A search through the Inorganic Crystal Structure Databank (ICSD) for similar cells yielded Fe_2PO_5. Comparison of its powder data (12) with those of the new phases indicated a close similar-

0022-4596/94 $6.00

TABLE 1
X-Ray Powder Diffraction Data for $LiTiPO_5$ and $LiTiAsO_5$

$LiTiPO_5$				$LiTiAsO_5$			
d_{obs} (Å)	d_{calc} (Å)	I/I_0	hkl	d_{obs} (Å)	d_{calc} (Å)	I/I_0	hkl
5.170	5.172	17	101	5.294	5.294	27	101
4.780	4.782	25	011	4.123	4.124	27	111
4.015	4.016	10	111	3.764	3.762	2	200
3.699	3.700	4	200	3.724	3.725	14	002
3.619	3.616	24	002	3.355	3.358	100	201
3.293	3.294	100	201	3.288	3.288	74	020
3.248	3.249	35	102	3.268	3.266	12	210
3.186	3.187	89	020	2.978	2.977	35	112
2.925	2.927	12	120	2.793	2.793	23	121
	2.926		211	2.648	2.647	3	202
2.894	2.895	16	112	2.377	2.377	1	301
2.712	2.713	18	121	2.345	2.343	37	122
2.586	2.586	7	202	2.323	2.323	16	013
2.414	2.415	5	220	2.103	2.103	2	031
	2.411		003	2.080	2.080	7	302
2.290	2.292	6	103	2.072	2.072	2	203
	2.290		221	2.060	2.062	1	222
2.275	2.275	25	122	2.025	2.025	5	131
2.255	2.255	12	013	1.983	1.984	6	312
2.191	2.192	4	311	1.977	1.977	1	213
2.157	2.157	7	113				
2.038	2.039	20	031				
	2.038		302				
2.020	2.020	10	203				
		+48 other lines		+38 other lines			
		a = 7.4000(5) Å		a = 7.5257(5) Å			
		b = 6.3752(3) Å		b = 6.5786(4) Å			
		c = 7.2347(4) Å		c = 7.4524(5) Å			

ity. The structure of Fe_2PO_5 (12) was then used as a starting model for Rietveld refinement, in which Li^+ was placed on Fe^{2+} sites and Ti^{4+} on Fe^{3+} sites. Final dimensions, (obtained after the Rietveld refinements) were a = 7.4000(5) Å, b = 6.3752(3) Å, c = 7.2347(4) Å for $LiTiPO_5$ and a = 7.5257(5) Å, b = 6.5786(4) Å, c = 7.4524(5) Å for $LiTiAsO_5$. Indexed powder X-ray diffraction data are given in Table 1.

Structure Refinement

The structure of $LiTiPO_5$ was refined in the orthorhombic space group *Pnma* (No. 62) (13), as in the Fe_2PO_5 structure refinement. At first, 13 profile parameters were allowed to refine, including 5 background coefficients, unit cell dimensions, scale factors, and 2θ zero-point. A squared Lorentzian function was used to describe the peak shape; this gave a good, although not perfect, fit to the data.

After convergence, the structural parameters were refined, first by refining the titanium positions, then each of the oxygens, followed by phosphorus, and finally lithium. When all the atomic positions had converged, the calculated profile was refined once more to allow for any slight modifications to the original model. The isotropic thermal vibration parameters were then refined in the same order as the positional parameters. However, it was found that the thermal parameters of O(2) and O(4) would not converge, and instead tended toward zero. To test whether the space group *Pnma* was perhaps inappropriate, the original model was modified slightly to allow refinement in the orthorhombic space group $Pn2_1a$ (No. 33) (13); this is similar to *Pnma*, but without a center of symmetry. The results of this test were unsatisfactory, however, as the y coordinates for O(1), O(2), and O(3) would not converge; this space group was discounted, therefore, and *Pnma* retained.

A similar procedure was used to refine the structure of the arsenate analogue, $LiTiAsO_5$; in this case, the isotropic thermal parameters, U_{iso}, refined satisfactorily for all atoms in the structure although the final values for O(2) and O(4) were very small, about 5–10 times less than

TABLE 2
Atomic Coordinates and Thermal Vibration Parameters for $LiTiAsO_5$

Atom	Wyckoff position	x/a	y/b	z/c	U_{iso}[a]	Occ.
Li	4a	0	0	0	0.0164	1
Ti	4c	0.334(1)	0.75	0.228(1)	0.0164	1
As	4c	0.375(1)	0.25	0.129(1)	0.0183	1
O(1)	4c	0.111(4)	0.75	0.158(4)	0.0167	1
O(2)	4c	0.806(4)	0.75	−0.002(4)	0.0044	1
O(3)	4c	0.067(4)	0.25	0.493(4)	0.0137	1
O(4)	8d	0.8775(3)	0.449(3)	0.226(2)	0.0016	1

[a] These parameters were fixed in the final refinement cycle; no ESDs are given, therefore.

for the other two oxygens. The U_{iso} values for all atoms were then fixed and a final refinement of the calculated profile and atomic coordinates was carried out.

The refined U_{iso} values for $LiTiAsO_5$ were assumed to be appropriate for $LiTiPO_5$ also. They were therefore inserted into the $LiTiPO_5$ model, fixed, and a final refinement of the calculated profile and positional parameters was carried out.

The final refinements for $LiTiAsO_5$ and $LiTiPO_5$ and R factors (14) of $R_p = 6.80\%$, $R_{wp} = 10.40\%$, $R_I = 13.92\%$ and $R_p = 3.83\%$, $R_{wp} = 5.66\%$, $R_I = 17.52\%$, respectively. Final atomic coordinates are given in Tables 2 and 3 with bond lengths and angles given in Tables 4 and 5; the fitted profiles are shown in Figs. 1 and 2.

Description of the $LiTiPO_5$, $LiTiAsO_5$ Structures

The structures of $LiTi(P,As)O_5$ are essentially isostructural with that of α-Fe_2PO_5[1] in that Li and Ti occupy Fe^{2+} and Fe^{3+} sites, respectively. The P/As atoms occupy tetrahedral sites that share corners with Li and Ti octahedral sites. The LiO_6 octahedra share opposite edges to form distorted infinite chains running parallel to b, as shown in [100] and [010] projections of parts of the structures in Figs. 3 and 4. Neighboring Li octahedral chains are separated by half a unit cell in both a and c directions and are rotated somewhat about the chain axis relative to each other, Fig. 4. The Li chains are connected, above and below, by chains of alternating corner-sharing TiO_6 octahedra and PO_4 tetrahedra, also running parallel to b; they are connected in such a way that the TiO_6 octahedra share two of their faces with adjacent LiO_6 octahedra in one of the Li chains.

The structure also contains chains of corner-sharing TiO_6 octahedra which run parallel to a, Fig. 3. The Ti atoms are displaced off-center from their octahedra, apparently as a direct consequence of the closeness of Li atoms in the octahedra with which they share faces. This displacement is reflected in a variation in Ti–O bond lengths, Tables 4 and 5.

The R_p and R_{wp} values from the Rietveld refinements are significantly greater for $LiTiAsO_5$ than for $LiTiPO_5$. Both phases were, however, slightly impure. In the $LiTiPO_5$ sample, small amounts of $LiTi_2(PO_4)_3$ and TiO_2 were detected, Fig. 1, perhaps caused by a volatilization of small amounts of Li_2O/P_2O_5 during reaction. In the $LiTiAsO_5$ sample, small amounts of β-Li_3AsO_4 and TiO_2 were detected, Fig. 2, probably caused by As_2O_5 volatilization. The presence of these impurity phases will have contributed to the final values of the R factors. Although the STOE refinement package permits exclusion of impurity regions, we have not done this, even though it would lead to a reduction in R values. The package does not

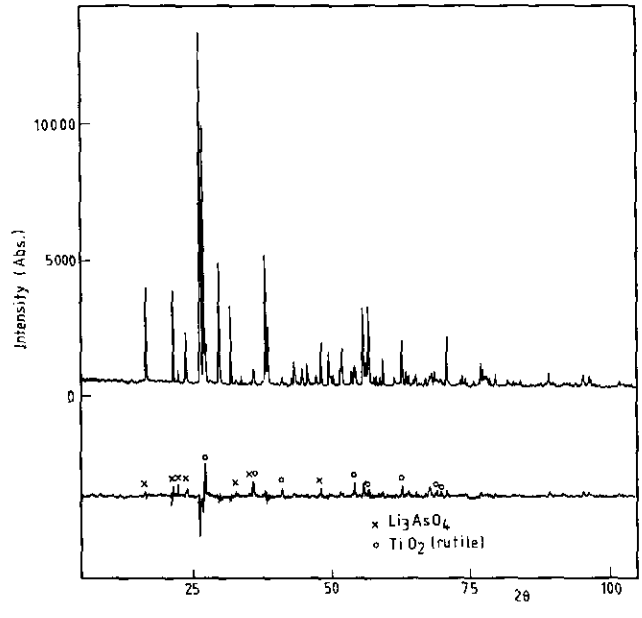

FIG. 1. X-ray diffraction profiles for $LiTiAsO_5$; difference plot is shown on the same scale.

[1] A low-temperature β-Fe_2PO_5 polymorph of a different structure also exists (20).

TABLE 3
Atomic Coordinates and Thermal Vibration Parameters for $LiTiPO_5$

Atom	Wyckoff position	x/a	y/b	z/c	U_{iso}[a]	Occ.
Li	4a	0	0	0	0.0164	1
Ti	4c	0.329(1)	0.75	0.220(1)	0.0164	1
P	4c	0.373(1)	0.25	0.125(1)	0.0183	1
O(1)	4c	0.107(3)	0.75	0.161(2)	0.0167	1
O(2)	4c	0.798(3)	0.75	−0.006(2)	0.0044	1
O(3)	4c	0.055(3)	0.25	0.487(2)	0.0137	1
O(4)	8d	0.873(2)	0.435(2)	0.243(2)	0.0016	1

[a] U_{iso} values were taken to be the same as refined $LiTiAsO_5$ values.

permit simultaneous refinement of two or more phases. The refined oxygen coordinates had much larger esds for $LiTiAsO_5$ than for $LiTiPO_5$ indicating, perhaps, a certain amount of positional/rotational disorder of the AsO_4 tetrahedra associated with the difficulty in accommodating the AsO_4 tetrahedra in the structure, since they are much larger than PO_4 tetrahedra.

Comparison of LiTi(P, As)O_5 Structures with Those of the Al_2SiO_5 Polymorphs

It was noted by Modaressi *et al.* (12) that the structure of Fe_2PO_5 had strong similarities to the structures of the kyanite and sillimanite polymorphs of Al_2SiO_5. Sillimanite also has space group *Pnma*, after interchanging axes (15), with chains of edge-sharing AlO_6 octahedra running parallel to *b*. Unlike the structures of Fe_2PO_5 and LiTi(P, As)O_5, however, the AlO_6 chains are linked by double chains of corner-sharing, alternate AlO_4 and SiO_4 tetrahedra; no face-sharing occurs.

The structure of kyanite is somewhat different yet again (16). It contains chains of edge-sharing octahedra, as in sillimanite but these are linked by chains of alternating AlO_6 octahedra and SiO_4 tetrahedra. The arrangement is not the same as in LiTi(P, As)O_5 and Fe_2PO_5, however, as no face sharing of octahedra occurs.

The structure of andalusite (17) bears the least resemblance to those of LiTi(P, As)O_5. Chains of edge-sharing, distorted AlO_6 octahedra are again present but the other Al atoms are in 5-coordinate, distorted trigonal bipyramidal sites. These latter polyhedra occur in edge-sharing pairs and corner-share with the SiO_4 tetrahedra, thus creating a framework which corner-shares with the Al octahedral chains.

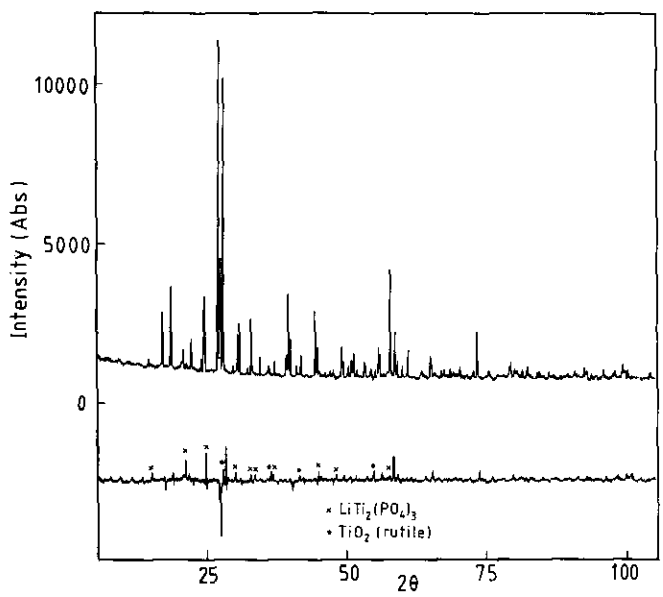

FIG. 2. X-ray diffraction profiles for $LiTiPO_5$; difference plot is shown on the same scale.

Electrical Properties of LiTi(P,As)O_5

The conductivities of sintered pellets of $LiTiPO_5$ and $LiTiAsO_5$ were measured using ac impedance techniques (17). The conductivities were very low, as summarized

TABLE 4
Bond lengths (in Å) for $LiTiAsO_5$ and $LiTiPO_5$

(a) $LiTiAsO_5$		(b) $LiTiPO_5$	
As–O(4) ×2	1.70(2)	P–O(4) ×2	1.52(1)
As–O(2)	1.66(3)	P–O(2)	1.53(2)
As–O(3)	1.71(3)	P–O(3)	1.57(2)
Mean:	1.69	Mean:	1.54
Li–O(4) ×2	1.95(2)	Li–O(4) ×2	2.04(1)
Li–O(1) ×2	2.19(2)	Li–O(1) ×2	2.13(1)
Li–O(2) ×2	2.20(2)	Li–O(2) ×2	2.19(1)
Mean:	2.07	Mean:	2.12
Ti–O(1)	1.76(3)	Ti–O(1)	1.70(2)
Ti–O(4) ×2	2.04(2)	Ti–O(4) ×2	2.05(1)
Ti–O(1)′	2.25(3)	Ti–O(1)′	2.23(2)
Ti–O(2)	2.06(3)	Ti–O(2)	2.08(2)
Ti–O(3)	1.90(3)	Ti–O(3)	1.89(2)
Mean:	2.00	Mean:	2.00

TABLE 5
Bond Angles for $LiTiAsO_5$ and $LiTiPO_5$

(a) $LiTiAsO_5$		(b) $LiTiPO_5$	
O(4)–As–O(4)′	101.0(10)	O(4)–P–O(4)′	102.1(8)
O(4)–As–O(2) ×2	111.8(11)	O(4)–P–O(2) ×2	110.7(9)
O(4)–As–O(3) ×2	109.4(11)	O(4)–P–O(3) ×2	109.1(9)
O(2)–As–O(3)	112.8(12)	O(2)–P–O(3)	114.5(9)
Mean:	109.4	Mean:	109.0
O(4)–Li–O(1) ×2	98.9(9)	O(4)–Li–O(1) ×2	98.5(5)
O(4)–Li–O(1) ×2	81.1(9)	O(4)–Li–O(1) ×2	81.5(5)
O(4)–Li–O(2) ×2	100.3(9)	O(4)–Li–O(2) ×2	98.8(5)
O(4)–Li–O(2) ×2	79.7(9)	O(4)–Li–O(2) ×2	81.2(5)
O(1)–Li–O(2) ×2	72.2(9)	O(1)–Li–O(2) ×2	73.8(6)
O(1)–Li–O(2)	107.8(9)	O(1)–Li–O(2) ×2	106.3(6)
Mean:	90.0	Mean:	90.0
O(4)–Ti–O(1) ×2	101.8(11)	O(4)–Ti–O(1) ×2	100.7(7)
O(4)–Ti–O(1) ×2	77.7(9)	O(4)–Ti–O(1) ×2	78.7(5)
O(4)–Ti–O(2) ×2	81.3(9)	O(4)–Ti–O(2) ×2	83.6(6)
O(4)–Ti–O(3) ×2	95.3(10)	O(4)–Ti–O(3) ×2	92.6(6)
O(1)–Ti–O(2)	101.4(11)	O(1)–Ti–O(2)	98.2(7)
O(1)–Ti–O(2)	73.6(10)	O(1)–Ti–O(2)	73.7(6)
O(1)–Ti–O(3)	96.0(12)	O(1)–Ti–O(3)	102.4(8)
O(1)–Ti–O(3)	89.0(10)	O(1)–Ti–O(3)	85.7(7)
Mean:	89.4	Mean:	89.3

briefly in Table 6. Since the crystal structures show no evidence of cation disorder or partial site occupancies, high ionic conductivities were not, in fact, expected. Attempts at doping to give either interstitial Li^+ ions or Li^+ vacancies were apparently unsuccessful; the products were not phase-pure by X-ray powder diffraction and showed only modest improvements in conductivity. It was not determined whether the charge carriers responsible for the low levels of conductivity were ions or electrons.

Subsolidus Phase Diagrams Li_2O–TiO_2–$(P, As)_2O_5$

During the study of the stoichiometry and stability of the new phases $LiTi(P, As)O_5$ and of $LiTi_2(PO_4)_3$, a considerable amount of data was accumulated on the subsolidus phase relationships in the ternary systems Li_2O–TiO_2–P_2O_5 and Li_2O–TiO_2–As_2O_5, from which the diagrams shown in Figs. 5 and 6 were constructed. Li_2O- and $(P, As)_2O_5$-rich corners of the diagrams were not determined. Composition studied are marked by circles, with indications as to whether the products were single phase or phase mixtures. Reaction temperatures were generally in the range 850–950°C, apart from P_2O_5-rich compositions which melted at these temperatures and were instead reacted at ~600°C. The results shown are deemed to represent equilibrium results since, for each, no changes in the products were observed either by using longer heating times or somewhat different reaction temperatures.

The phase diagram Li_2O–TiO_2–P_2O_5, Fig. 5, shows two ternary phases, $LiTi_2(PO_4)_3$ and $LiTiPO_5$; both appear to be stoichiometric line phases. In particular, no evidence for solid solution formation by $LiTi_2(PO_4)_3$ was found. In

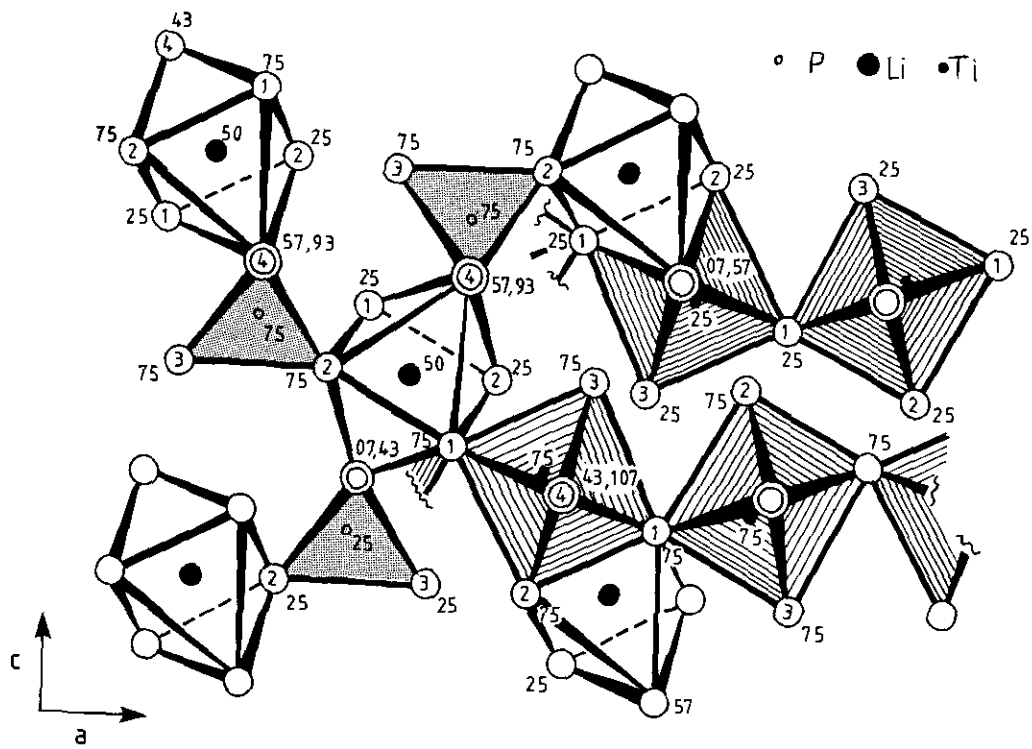

FIG. 3. [010] projection of the structures of $LiTi(P, As)O_5$; PO_4 tetrahedra are stippled; TiO_6 octahedra are striped.

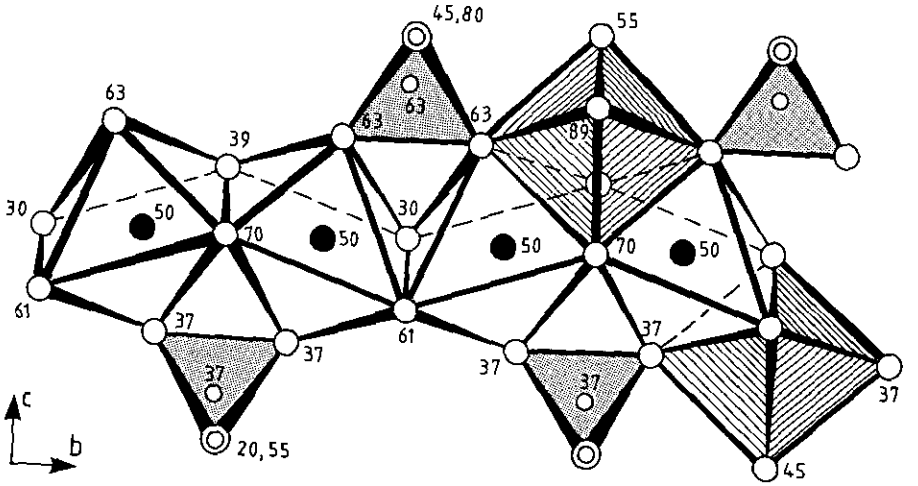

FIG. 4. [100] projection of the structures of LiTi(P, As)O_5.

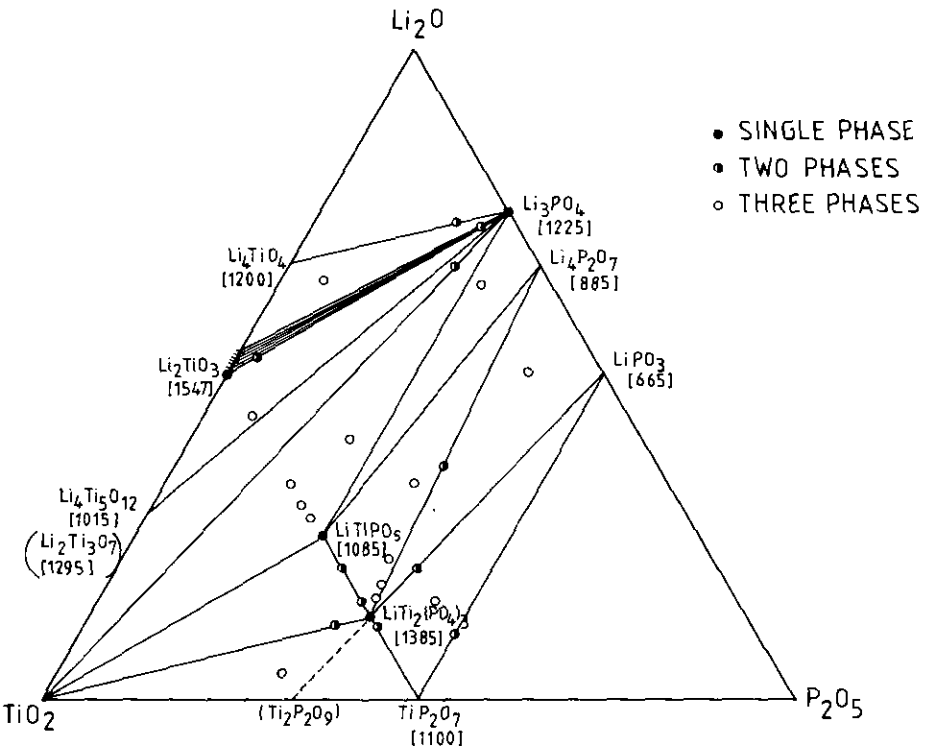

FIG. 5. Subsolidus phase relations in the system Li_2O–TiO_2–P_2O_5 at ~600–900°C. Melting temperatures of phases shown in brackets.

TABLE 6
Conductivity results

Composition	Sintering conditions	E_a (eV)	σ at 400°C (S cm^{-1})
$LiTiPO_5$	1000°C, 2 hr	1.00(11)	1.1×10^{-5}
$Li_{1+x}TiP_{1-x}Si_xO_5$[a] ($x = 0.1$)	1065°C, 1 hr	1.26(13)	1.5×10^{-5}
$Li_{1-x}Ti_{1-x}Nb_xPO_5$[a] ($x = 0.1$)	1065°C, 1 hr	0.94(8)	1.2×10^{-5}
$LiTiAsO_5$	1055°C, 1 hr	1.19(10)	5×10^{-7}
$Li_{1+x}TiAs_{1-x}Ge_xO_5$[a] ($x = 0.1$)	940°C, 1 hr	1.00(10)	3×10^{-6}
$Li_{1-x}Ti_{1-x}Nb_xAsO_5$[a] ($x = 0.1$)	1055°C, 1 hr	1.06(15)	5.5×10^{-6}

[a] All compositions other than stoichiometric $LiTiPO_5$ and $LiTiAsO_5$ were phase mixtures after reaction.

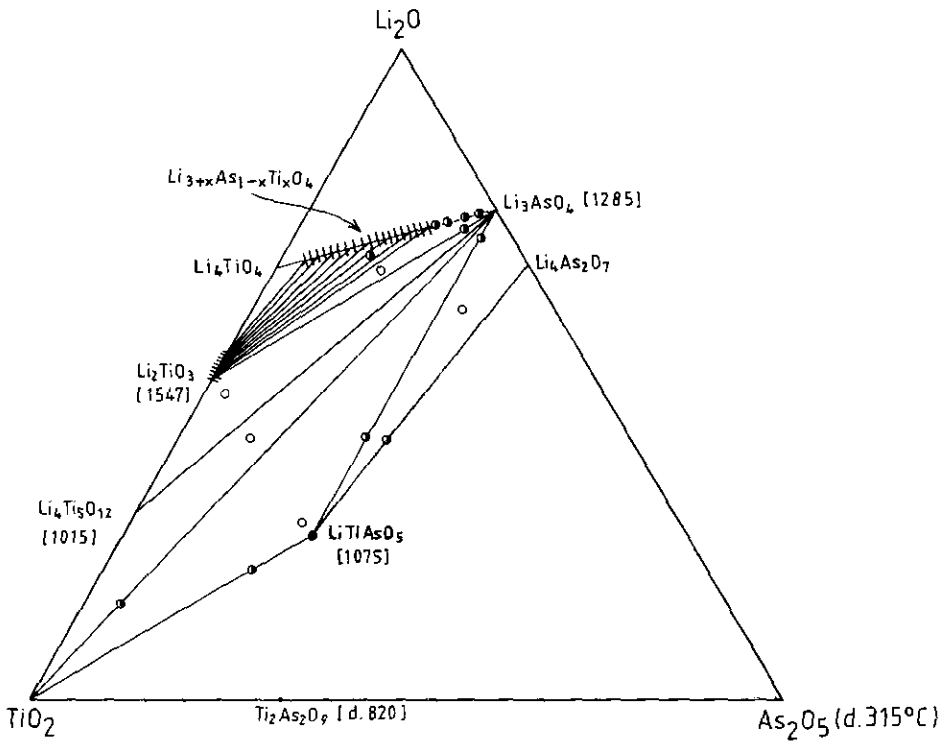

FIG. 6. Subsolidus phase relations in the system Li_2O–TiO_2–As_2O_5 at ~600–900°C.

the phase diagram Li_2O–TiO_2–As_2O_5, Fig. 6, there was no evidence for the arsenate analogue of $LiTi_2(PO_4)_3$: compositions in this region had very low melting temperatures and are excluded from consideration in Fig. 6. A range of γ solid solutions of general formula $Li_{3+x}As_{1-x}Ti_xO_4$: $0.225 < x < 0.8$ is present on the diagram. A detailed study of these solid solutions and their electrical properties has been given (18). Similar γ solid solutions appear not to form in the corresponding phosphate system.

ACKNOWLEDGMENTS

We thank the SERC for financial support, the International Centre for Diffraction Data for a scholarship (J.M.S.S.), and SERC for use of the Chemical Database Service at Daresbury.

Note. Since this work was completed and submitted for publication, a paper has appeared concerning the preparation and structure of the lithium titanium double phosphate, $LiTiOPO_4$ (19). The structure was determined by single crystal X-ray diffraction on a sample crystallized from a melt of $Li_2O \cdot P_2O_5$ saturated with TiO_2 at 1100°C. The structure was solved by direct methods. There is good agreement between our data, including atomic coordinates, bond lengths and angles, and those given in Ref. (19). Most parameters agree to within two esds for the two structure determinations.

REFERENCES

1. S-C. Li and Z-X. Lin, *Solid State Ionics* **9 & 10,** 835 (1983).
2. M. A. Subramanian, R. Subramanian, and A. Clearfield, *Solid State Ionics* **18 & 19,** 562 (1986).
3. Z-X. Lin, H-J. Yu, S-C. Li, and S-B. Tian, *Solid State Ionics* **31,** 91 (1988).
4. H. Aono, E. Sugimato, Y. Sadaoka, N. Imanaka, and G. Adachi, *J. Electrochem. Soc.* **136,** 590 (1989).
5. H. Aono, E. Sugimato, Y. Sadaoka, N. Imanaka, and G. Adachi, *Chem. Lett.* 331 (1990).
6. H. Aono, E. Sugimato, Y. Sakaoka, N. Imanaka, and G. Adachi, *J. Electrochem. Soc.* **137,** 4 (1990).
7. H. Aono, E. Sugimato, Y. Sakaoka, N. Imanaka, and G. Adachi, *Solid State Ionics* **47,** 257 (1991).
8. H. Aono, E. Sugimato, G. Sakaoka, N. Imanaka, and G. Adachi, "Proceedings 8th International Conference Solid State Ionics," 1991.
9. N. Machida, K. Fuju, and T. Minami, *Chem. Lett.* **3,** 367 (1991).
10. G. Ando, N. Hirose, J. Kuwano, M. Kato, and H. Ohtsuka, *Phosphorous Res. Bull.* **1,** 239 (1991).
11. K. Ado, Y. Saito, T. Asai, H. Kageyama, and O. Nakamura, *Solid State Ionics* **53–56,** 723 (1992).
12. A. Modaressi, A. Courtois, R. Gerardin, B. Maldman, and C. Glietzer, *J. Solid State Chem.* **40,** 301 (1981).
13. T. Hahn (Ed.), "International Tables for Crystallography," Vol. A. Reidel, Dordrecht/Boston, 1983.
14. H. M. Rietveld, *J. Appl. Crystallogr.* **2,** 65 (1969).
15. C. Burnham, *Z. Kirstallogr.* **118,** 127 (1963).
16. C. Burnham, *Z. Kristallogr.* **118,** 337 (1963).
17. C. Burnham and M. Buerger, *Z. Kristallogr.* **115,** 269 (1961).
18. A. R. Rodger, J. Kuwano, and A. R. West, *Solid State Ionics* **15,** 185 (1985).
19. P. G. Nagornyi, A. A. Kapshuk, N. V. Stus, N. S. Slobodyanik, and A. N. Chernega, *Russ. J. Inorg. Chem.* **36**(11), 2766 (1991).
20. M. Izzaali, B. Malaman, C. Gleitzer, J. K. Warner, J. A. Hriljac, and A. K. Cheetham, *J. Solid State Chem.* **86,** 195 (1990).